

Article

Investigation on Film Quality and Photophysical Properties of Narrow Bandgap Molecular Semiconductor Thin Film and Its Solar Cell Application

Xiaotong Li , Xiaoping Zou ^{*}, Chunqian Zhang, Jin Cheng, Guangdong Li, Yifei Wang, Xiaolan Wang, Keke Song, Baokai Ren and Junming Li 

Beijing Advanced Innovation Center for Materials Genome Engineering, Research Center for Sensor Technology, Beijing Key Laboratory for Sensor, Beijing Key Laboratory for Optoelectronic Measurement Technology, MOE Key Laboratory for Modern Measurement and Control Technology, School of Applied Science, Beijing Information Science and Technology University, Jianxiangqiao Campus, Beijing 100101, China; xiaotong252240@163.com (X.L.); chunqiancool@163.com (C.Z.); chengjin@bistu.edu.cn (J.C.); LGD1511455720@163.com (G.L.); yifewang2020@126.com (Y.W.); wangxl1105@163.com (X.W.); songmengke163@163.com (K.S.); brenbk2021@163.com (B.R.); li@bistu.edu.cn (J.L.)

^{*} Correspondence: xpzou2021@bistu.edu.cn; Tel.: +86-010-64884673

Abstract: Hexane-1,6-diammonium pentaiodobismuth (HDA-BiI₅) is one of the narrowest bandgap molecular semiconductor reported in recent years. Through the study of its energy band structure, it can be identified as an N-type semiconductor and is able to absorb most of the visible light, making it suitable to fabricate solar cells. In this paper, SnO₂ was used as an electron transport layer in HDA-BiI₅-based solar cells, for its higher carrier mobility compared with TiO₂, which is the electron transport layer used in previous researches. In addition, the dilution ratio of SnO₂ solution has an effect on both the morphology and photophysical properties of HDA-BiI₅ films. At the dilution ratio of SnO₂:H₂O = 3:8, the HDA-BiI₅ film has a better morphology and is less defect inside, and the corresponding device exhibited the best photovoltaic performance.

Keywords: molecular semiconductor; solar cell; SnO₂; thin film



Citation: Li, X.; Zou, X.; Zhang, C.; Cheng, J.; Li, G.; Wang, Y.; Wang, X.; Song, K.; Ren, B.; Li, J. Investigation on Film Quality and Photophysical Properties of Narrow Bandgap Molecular Semiconductor Thin Film and Its Solar Cell Application. *Coatings* **2021**, *11*, 1300. <https://doi.org/10.3390/coatings11111300>

Academic Editor: Je Moon Yun

Received: 18 September 2021

Accepted: 18 October 2021

Published: 27 October 2021

Publisher's Note: MDPI stays neutral with regard to jurisdictional claims in published maps and institutional affiliations.



Copyright: © 2021 by the authors. Licensee MDPI, Basel, Switzerland. This article is an open access article distributed under the terms and conditions of the Creative Commons Attribution (CC BY) license (<https://creativecommons.org/licenses/by/4.0/>).

1. Introduction

In recent years, solar cells have achieved rapid development, especially the third-generation solar cells [1–3]. Researchers have also started to experiment with various new materials to develop solar cells with better performance [4–6]. The molecular semiconductor with the narrowest bandgap of 1.89 eV, hexane-1,6-diammonium pentaiodobismuth (HDA-BiI₅), was reported by Zhang et al. in 2017 and was concluded to be an indirect bandgap semiconductor [7]. It was also reported in 2016 as a hybrid organic-inorganic material by Fabian et al. [8]. They identified HDA-BiI₅ as an N-type semiconductor by its energy band structure. With the narrow bandgap, HDA-BiI₅ is able to absorb most of the ultraviolet-visible (UV-vis) light from sunlight, making it more suitable than other molecular semiconductors for use as a light absorption layer in solar cells.

Up to now, two types of HDA-BiI₅-based photovoltaic devices have been reported. Fabian et al. [8] used a mesoporous structure with TiO₂ and 2,2',7,7'-tetrakis(N,N'-di-p-methoxyphenyl-amine)9,9'-spirofluorene (Spiro-MeOTAD) as the electron transport layer (ETL) and the hole transport layer (HTL), respectively. A photocurrent of 0.124 mA/cm² and a power conversion efficiency (PCE) of 0.027% were obtained. Liu et al. [9] prepared HDA-BiI₅-based solar cells with only TiO₂ as the ETL and no HTL in 2020. They realized an open-circuit voltage (V_{oc}) of 0.55 V and a short-circuit current density (J_{sc}) of 17.5 μA/cm². The value of PCE is not given, but according to the current-voltage (J-V) curve, it is an order of magnitude lower than that of Fabian et al. A comparison revealed that only one

material, TiO₂, had been tried for the electron transport layer, and perhaps the devices could be optimized from this aspect.

SnO₂ has a higher carrier mobility than that of TiO₂, [10,11], which may be able to improve the device performance, forming better interfacial contact and efficient transport of photo-generated electrons [12,13]. In this paper, the energy band structure of HDA-BiI₅ thin films, as well as their film morphology and photophysical properties on ITO/SnO₂ substrates, are investigated in detail. In addition, whether the dilution ratio of SnO₂ to H₂O during the preparation of the SnO₂ layer has any effect on the morphology and photophysical properties of HDA-BiI₅ films was carried out, [14–19] and the corresponding solar cells were fabricated.

2. Materials and Methods

2.1. Preparation of Device

To start, 100 mL of HI solution was mixed with 5.9 g (10.0 mmol) of BiI₃ powder in a round bottom flask and was stirred for about 1 h at room temperature on a temperature-controlled digital magnetic stirrer to dissolve it fully. After the internal temperature reached 90 °C and stabilized, 1.16 g (10.0 mmol) of 1,6-hexanediamine crystals was added and stirred magnetically while heating for 12 h to dissolve and react with 1,6-hexanediamine crystals. After that, the solution in the flask was poured into a clean beaker and placed on an intelligent temperature-controlled baking table, and the solution in the beaker was slowly evaporated and crystallized at 90 °C until dark red crystals. HDA-BiI₅ crystals were precipitated at the bottom of the beaker. The crystals were scraped from the beaker with a glass rod, grinded into a powder, and placed into a small glass vial, which was then sealed with a sealant and kept as a reserve.

Indium tin oxide (ITO) was selected as the substrate and cleaned using detergent, isopropanol and acetone mixture, ethanol, and deionized water in turn. Regarding the preparation of SnO₂ ETL, 300 µL of SnO₂ solution was mixed with 600, 800, 1000, 1200, and 1400 µL of ultrapure water to make up a solution with dilution ratios of 3:6, 3:8, 3:10, 3:12 and 3:14, respectively. It was then mixed well by ultrasonication. The five different dilution ratios of SnO₂ solutions were spin-coated onto the conductive substrates at a rate of 4000 rpm for 30 s. Immediately after spin-coating, the films were annealed on a hot plate at 150 °C for 30 min. UV ozonation was performed for 15 min after annealing to provide a better hydrophilic surface for the spin-coating of the light absorption layer.

In the preparation of HDA-BiI₅ films, 500 mg of stored HDA-BiI₅ powder was taken out and poured into a small clean transparent glass vial, followed by 0.4 mL of DMF solution as solvent. The glass vial with the solution was put into the ultrasonic cleaning equipment for 3 h until the powder was completely dissolved in the DMF solvent, and then the solution was filtered with a 0.22-µm-diameter filter nozzle to complete the preparation of HDA-BiI₅ precursor solution. Next, 40 µL of HDA-BiI₅ precursor solution was uniformly coated on the ITO/SnO₂ substrate, and spun for 40 s at a rate of 6000 rpm. Immediately after spin-coating, it was annealed on a hot plate at 150 °C for 30 min. After annealing, the HDA-BiI₅ light absorption layer was also prepared.

The HTL was prepared using the directly purchased Spiro-MeOTAD spin-coating solution. Then, 20 µL of Spiro-MeOTAD spin-coating solution was pipetted and spin-coated at 3000 rpm for 30 s. After spin-coating, it was annealed on a hot plate at 60 °C for 8 min. Finally, an 80-nm-thick gold electrode was thermally evaporated on the HTL. The effective area of the prepared photovoltaic devices was 0.2 × 0.2 cm².

2.2. Characterization

The surface morphology of HDA-BiI₅ thin films was characterized by scanning electron microscope (SIGMA, Zeiss, Jena, Germany). The X-ray diffraction (XRD) patterns were obtained from X-ray diffractometer (D8 focus, Bruker, Dresden, Germany) with Cu radiation ($\lambda = 1.5418 \text{ \AA}$) at 40 kV, 40 mA. Energy dispersive X-ray spectroscopy (EDS) was used to analyze the elemental composition of the film. Ultraviolet photoemission

spectroscopy (UPS) was used to determine the electronic band structure of the HDA-BiI₅ thin film. A photoluminescence spectrometer (FluoroMax-Plus, HORIBA Scientific, Paris, France) was applied to obtain the photoluminescence spectra (PL) of light absorption layer films at 370 nm. The current–voltage (*J*–*V*) curve of the solar cells was measured by using a solar simulator and an electrochemical workstation (Oriel, Newport, RI, USA) under air-mass (AM) 1.5 sunlight.

3. Results and Discussion

The morphology of HDA-BiI₅ films prepared on SnO₂ layers spin-coated with five dilution ratios is shown in Figure 1. As can be seen from the figures, when the SnO₂/H₂O dilution ratio is 3:6, there are a lot of cracks and holes on the surface of HDA-BiI₅ film, and the grain boundaries cannot be obviously distinguished. Such cracks and holes may make contact between the hole transport layer and the electron transport layer in solar cells, resulting in electrical leakage. When the ratio SnO₂:H₂O = 3:8 is used to prepare the SnO₂ layer, the grain boundaries of HDA-BiI₅ thin film are obvious, and the surface is smooth with no obvious cracks. Although there are still a few holes, they are relatively small, illustrating that the film quality is improved. When the SnO₂/H₂O dilution ratio is 3:10, obvious cracks and large holes appear again on the surface of the HDA-BiI₅ film, and the grain boundaries become blurred. After continuously adjusting the dilution ratio to 3:12 and 3:14, the cracks and holes on the surface of the HDA-BiI₅ film continue to increase and increase, making it difficult to distinguish single crystal particles.

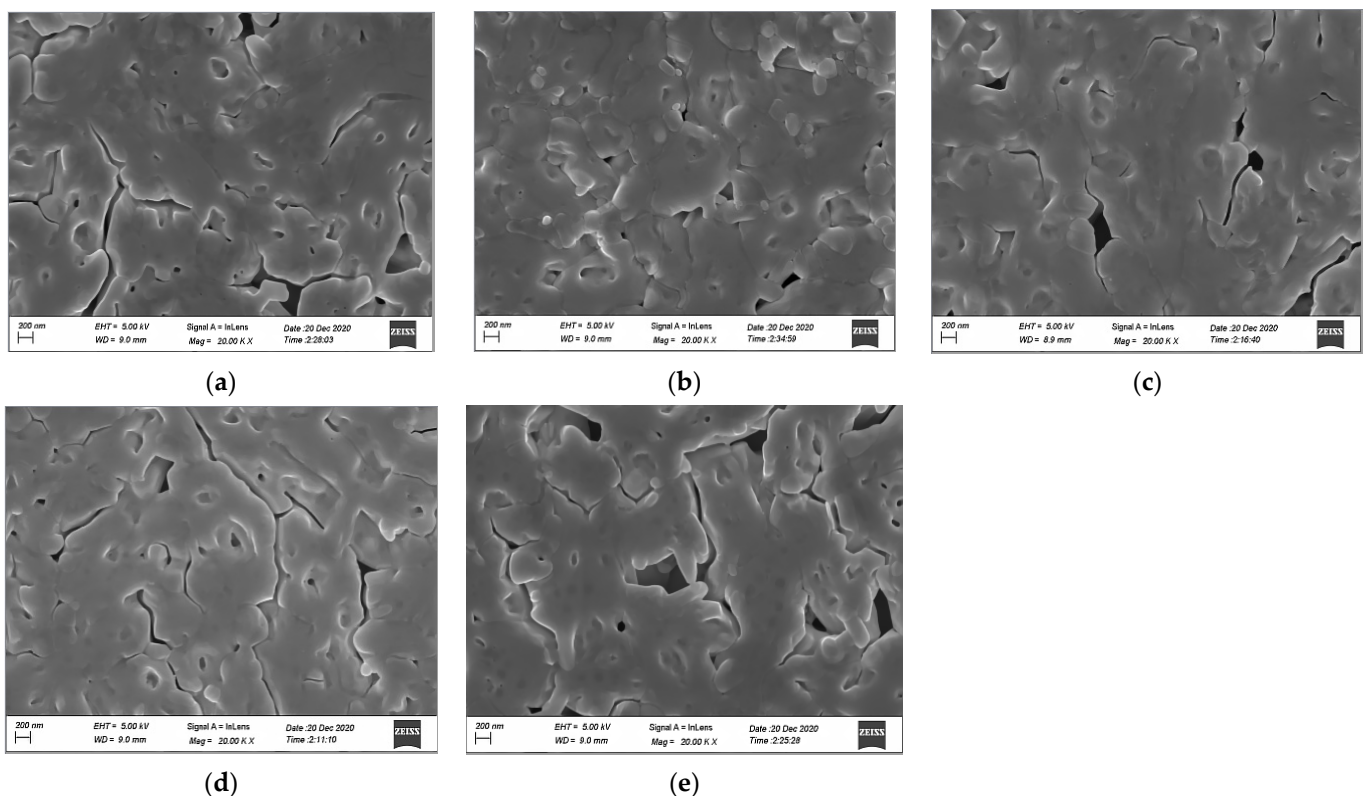


Figure 1. Scanning electron microscopy of HDA-BiI₅ thin films on electron transport layers prepared with different dilution ratios of SnO₂ and H₂O: (a) SnO₂:H₂O = 3:6, (b) SnO₂:H₂O = 3:8, (c) SnO₂:H₂O = 3:10, (d) SnO₂:H₂O = 3:12, (e) SnO₂:H₂O = 3:14.

Figure 2 shows XRD patterns of HDA-BiI₅ thin films deposited on “Glass/ITO/SnO₂” substrates. The main diffraction peak locations and corresponding crystal planes marked in the figure are basically consistent with the XRD characteristics of the HDA-BiI₅ thin films reported by Fabian et al. [8] and Zhang et al. [7], constituting a primitive orthorhombic crystal structure of space group Pna2₁, a = 15.1729(11), b = 14.3521(13), c = 8.6623(7) Å (at

296 K) [7]. It can be seen from the figure that the XRD characteristic curves of HDA-BiI₅ thin films on SnO₂ layers prepared with five dilution ratios are similar, which indicates that the lattice structure of the thin films was not changed. In addition, with the dilution ratio of SnO₂ to H₂O from 3:6 to 3:8, the peak strength slightly increases and reaches the highest at the ratio of 3:8, and then it slightly decreases as the ratio continues to change to 3:10, 3:12, and 3:14. This indicates that the crystallinity of the HDA-BiI₅ thin film prepared when the dilution ratio of SnO₂ to H₂O is 3:8 is the best, which is also consistent with the morphology characteristics of the HDA-BiI₅ thin film observed in Figure 1.

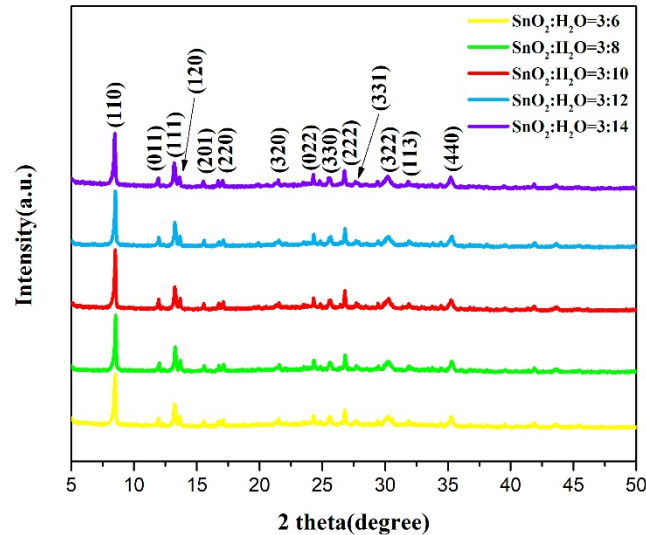


Figure 2. XRD patterns of HDA-BiI₅ thin films deposited on “Glass/ITO/SnO₂” substrates, where the SnO₂ layers are prepared with different dilution ratios.

The best quality film deposited on the “Glass/ITO/SnO₂” substrate with SnO₂:H₂O = 3:8 in Figure 1b was analyzed by EDS, as shown in Figure 3 below. The presence of each element of the HDA-BiI₅ in the energy spectrum can be seen from the figure, which, together with the XRD results, verifies the accuracy of the prepared HDA-BiI₅ films. In addition, the presence of Sn elements may be due to the ITO substrate and the SnO₂ layer.

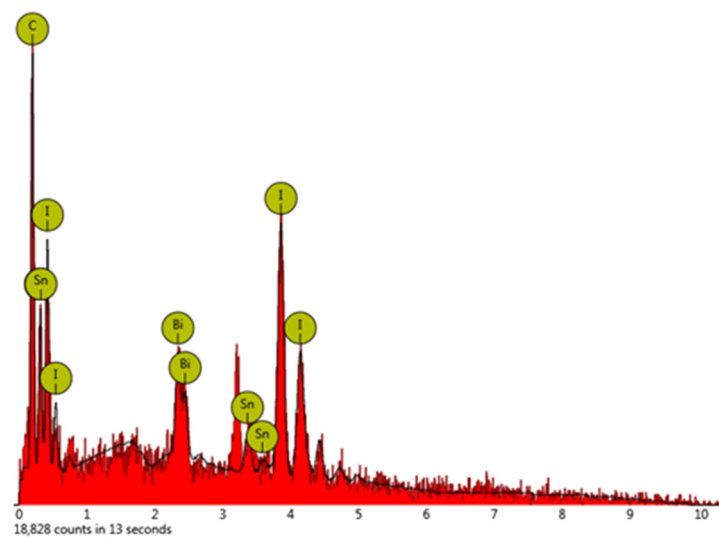


Figure 3. EDS patterns of HDA-BiI₅ thin films on Glass/ITO/SnO₂ substrates at SnO₂:H₂O = 3:8 dilution ratio.

Figure 4 shows the ultraviolet-visible (UV-vis) absorption spectra of the HDA-BiI₅ films on SnO₂ layers prepared with SnO₂ and H₂O in five dilution ratios of 3:6, 3:8, 3:10, 3:12, and 3:14, respectively. The photo absorption range of the HDA-BiI₅ films prepared on the five different SnO₂ layers is basically the same, and the corresponding Tauc plot shows that the bandgap of the HDA-BiI₅ material in our experiment is about 1.94 eV, which is close to the previously reported 1.89 eV [7].

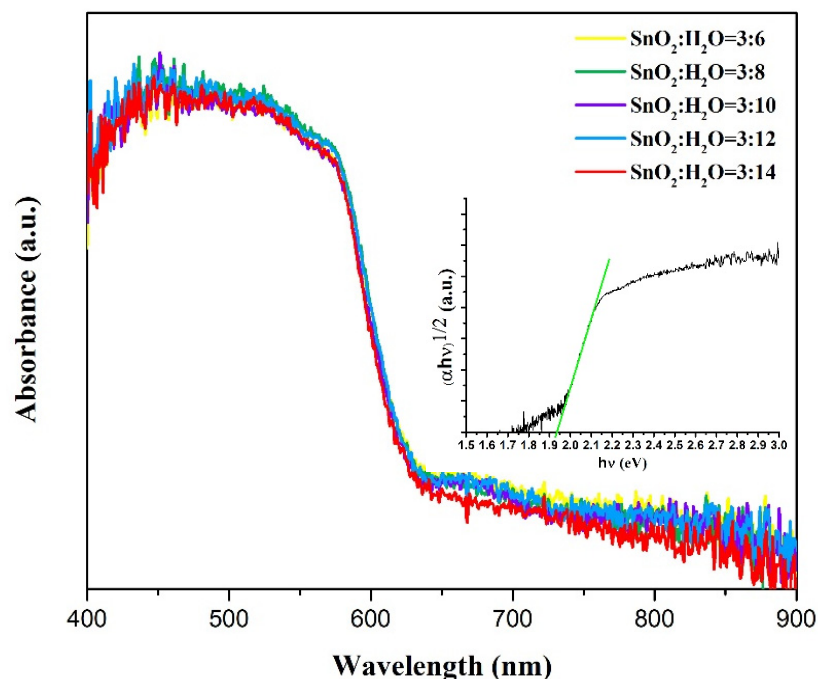


Figure 4. Ultraviolet-visible (UV-vis) absorption spectra of HDA-BiI₅ films prepared on SnO₂ layer prepared at five dilution ratios (inset: Tauc plot).

The energy band structure of HDA-BiI₅ thin film was measured by UPS, as shown in Figure 5. The Fermi energy level is corrected to 0 eV using a gold standard sample, and a bias voltage of −10 eV is applied to test the power function. The power function is calculated as follows in Equation (1).

$$\varphi_s = hv - (E_{cutoff} - E_F) = hv - E_{cutoff} + E_F \quad (1)$$

where hv is the excitation source energy, the HeII UV source used in this experiment is 21.22 eV; E_{cutoff} is the cutoff binding energy, as seen in the left figure; the cutoff binding energy is 16.21 eV; and E_F is the Fermi energy level, which was corrected to 0 eV during the test, so the calculated work function of HDA-BiI₅ is 5.01 eV. In order to further determine the valence band maximum (VBM) position of the material, tangent lines are made in the right figure, as shown in the red line, and the binding energy at the intersection point is 1.57 eV. Therefore, the VBM of the material is −6.58 eV. Based on the band gap of the material obtained from the absorption spectrum, the conduction band bottom of the material can be calculated as −4.64 eV, and its Fermi energy level is −5.01 eV which is closer to the CBM, indicating that the material is an N-type semiconductor. Although both are identified as N-type semiconductors, the VBM of HDA-BiI₅ in this paper differs from the data reported in 2016 by nearly 1 eV. The measured optical bandgap of the material also differs from the 2.1 eV reported in 2016 and the 1.89 eV in 2017. In particular, the CBM of HDA-BiI₅ in Fabian et al.'s research is higher than that of TiO₂ so that electrons can smoothly transport from HDA-BiI₅ to TiO₂; however, in this experiment, the calculated CBM of HDA-BiI₅ is lower than that of SnO₂, so there can be a potential barrier for electron

transport from the light absorption layer to the ETL. Furthermore, among the commonly used materials for electron transport, there are none that can match the -4.64 eV CBM.

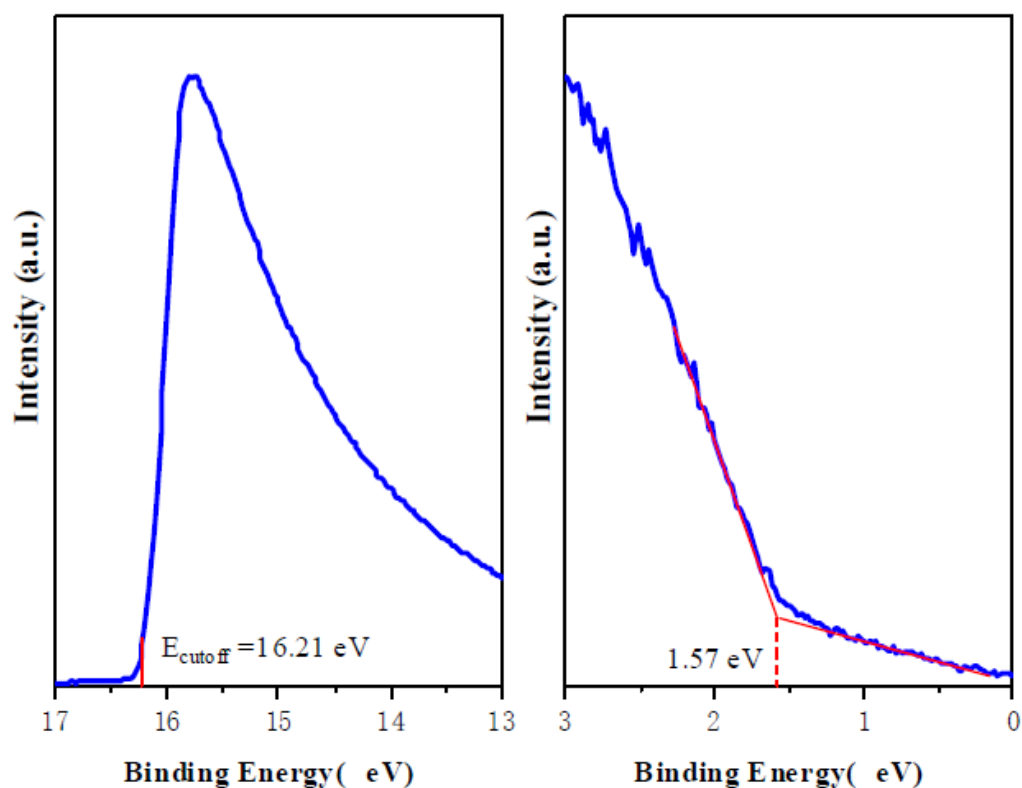


Figure 5. Ultraviolet photoemission spectra of HDA-BiI₅ films.

Figure 6 shows the photoluminescence spectra of HDA-BiI₅ films prepared on “Glass/ITO/SnO₂” substrates at the different dilution ratio of SnO₂ to H₂O. The excitation wavelength of the test is 370 nm and the scanning wavelength is between 450 and 850 nm. The main emission peaks of the films can be seen in the range of 500 to 700 nm, mainly due to the semiconductor bandgap luminescence, while other reasons, such as surface defects, may be responsible for the other lower emission peaks. When the dilution ratio of SnO₂ to H₂O is 3:8, the PL peaks of the prepared HDA-BiI₅ films are the lowest. Combined with the SEM morphology of the HDA-BiI₅ films at SnO₂: H₂O = 3:8, the morphology of the film is the best among the five species, and the defects in the film are correspondingly less, so the recombination of the photogenerated carriers in the PL test are the least, illustrating the forming of a better charge transportation between the HDA-BiI₅ film and the SnO₂ layer among the five cases. After that, with the increase in the proportion of H₂O in the SnO₂ solution, the PL peak of the HDA-BiI₅ film becomes higher again. Combined with the analysis of the SEM diagram in Figure 1, it may be that the lower the concentration of the SnO₂ solution diluted, the poorer the quality of the formed SnO₂ layer, the sparser the crystal growth, and the rougher the surface, which in turn leads to the poor quality of the HDA-BiI₅ film and the increase in the internal defects, making the exciton radiation recombination increase, and the electron generated in HDA-BiI₅ layer cannot be effectively transferred into the SnO₂ electron transport layer.

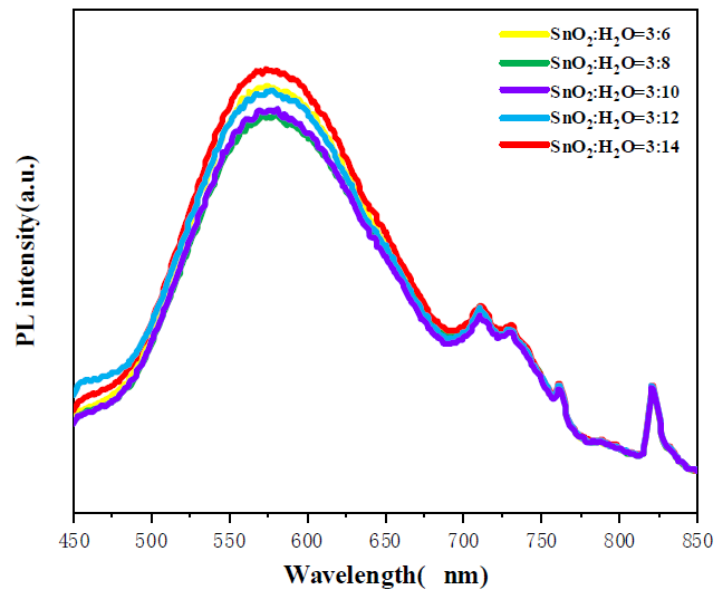


Figure 6. Photoluminescence spectra of HDA-BiI₅ films on glass/ITO/SnO₂ substrates at five SnO₂ to H₂O dilution ratios.

The corresponding solar cells were fabricated using different SnO₂ precursor solution concentrations; their *J-V* curves are shown in Figure 7. Consistent with the studies on the film quality and photophysical properties above, the photovoltaic performance of the devices also reached the maximum at SnO₂:H₂O = 3:8; the photovoltaic parameters are shown in detail in Table 1. The distribution of the performance parameters of the other devices we prepared with a dilution ratio of SnO₂:H₂O = 3:8 is shown in Figure 8, where the parameters are relatively close to each other, as seen in Table 2, proving the reliability and reproducibility of the study results. Further work can be carried out to improve the device performance by reducing energy level mismatches, such as using composite ETL and other preparation methods of SnO₂ [20–22].

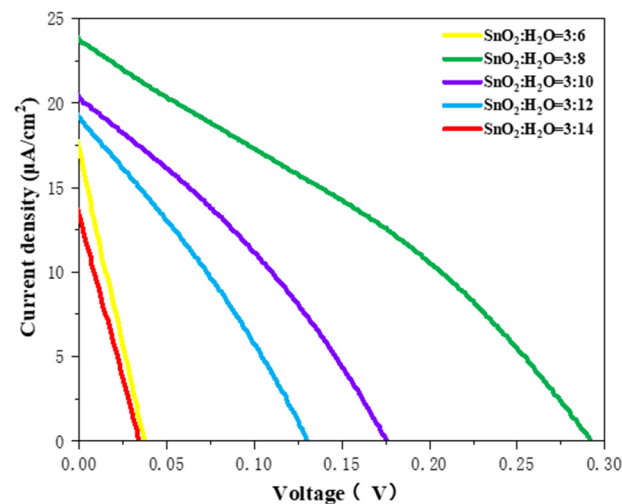
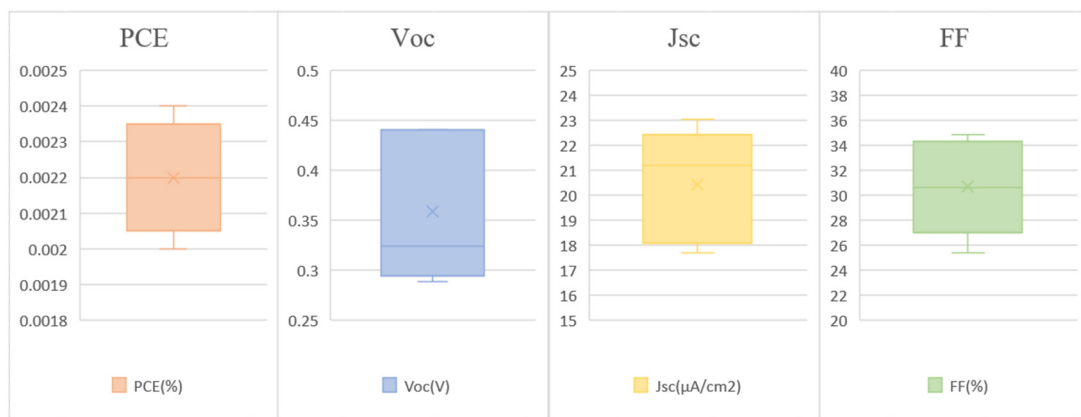


Figure 7. Forward scanning *J-V* curve of photovoltaic devices with HDA-BiI₅ as the light absorption layer, where the ETL is prepared at different dilution ratios.

Table 1. Photovoltaic performance parameters of solar cells fabricated with different dilution ratio of SnO₂ to H₂O.

SnO ₂ :H ₂ O	PCE (%)	Voc (V)	Jsc (μA/cm ²)	FF (%)
3:6	0.0002	0.04	15.02	30.52
3:8	0.0024	0.30	23.03	34.82
3:10	0.0013	0.18	19.40	37.26
3:12	0.0008	0.14	19.84	30.46
3:14	0.0001	0.03	13.44	32.01

**Figure 8.** Distribution of performance parameters of five HDA-BiI₅-based solar cells prepared with SnO₂:H₂O = 3:8.**Table 2.** Photovoltaic parameters for the five devices fabricated at 3:8 dilution ratios.

PCE (%)	Voc (V)	Jsc (μA/cm ²)	FF (%)
0.0024	0.3	23.03	34.82
0.0021	0.2889	21.2	33.8468
0.0023	0.4395	18.5	28.6934
0.002	0.4407	17.7	25.4019
0.0022	0.3242	21.8	30.6429

4. Conclusions

In this paper, HDA-BiI₅ thin films were prepared on ITO/SnO₂ substrates, and the film quality, energy band structure, and photophysical properties of the films were investigated in detail. It was found that its conduction band minimum was -4.64 eV, which does not match well with any of the widely used electron transport materials, which is a problem to be solved in the application of HDA-BiI₅ in photovoltaic field. In addition, the dilution ratio of SnO₂ to H₂O in the preparation of SnO₂ layers can affect the morphology and photophysical properties of HDA-BiI₅ films. The corresponding solar cells also exhibited the best performance at the 3:8 dilution ratio, showing a PCE of $0.0022 \pm 0.0002\%$. This work can provide references and ideas for the selection and optimization of ETL in the fabrication of HDA-BiI₅-based solar cells.

Author Contributions: Conceptualization, J.L. and C.Z.; methodology, G.L.; software, J.C.; validation, X.Z.; formal analysis, G.L. and X.L.; investigation, X.L.; resources, G.L.; data curation, X.L. and Y.W.; writing—review and editing, X.L.; visualization, X.W., K.S. and B.R.; supervision, X.Z.; funding acquisition, X.Z. All authors have read and agreed to the published version of the manuscript.

Funding: This work was supported by the National Natural Science Foundation of China (No. 61875186 and No. 61901009), State Key Laboratory of Advanced Optical Communication Systems Networks of China (2021GZKF002) and Beijing Key Laboratory for Sensors of BISTU (No. 2019CGKF007).

Institutional Review Board Statement: Not applicable.

Informed Consent Statement: Not applicable.

Data Availability Statement: Data is contained within the article.

Conflicts of Interest: The authors declare no conflict of interest.

References

1. Kim, G.; Min, H.; Lee, K.S.; Lee, D.Y.; Yoon, S.M.; Seok, S.I. Impact of strain relaxation on performance of alpha-formamidinium lead iodide perovskite solar cells. *Science* **2020**, *370*, 108–112. [[CrossRef](#)]
2. Wu, T.H.; Qin, Z.Z.; Wang, Y.B.; Wu, Y.Z.; Chen, W.; Zhang, S.F.; Cai, M.L.; Dai, S.Y.; Zhang, J.; Liu, J.; et al. The main progress of perovskite solar cells in 2020–2021. *Nano-Micro Lett.* **2021**, *13*, 152. [[CrossRef](#)]
3. Zhao, W.J.; Xu, J.; He, K.; Cai, Y.; Han, Y.; Yang, S.M.; Zhan, S.; Wang, D.P.; Liu, Z.K.; Liu, S.Z. A special additive enables all cations and anions passivation for stable perovskite solar cells with efficiency over 23%. *Nano-Micro Lett.* **2021**, *13*, 169. [[CrossRef](#)]
4. Hu, Y.Q.; Shan, Y.S.; Yu, Z.L.; Sui, H.J.; Qiu, T.; Zhang, S.F.; Ruan, W.; Xu, Q.F.; Jiao, M.M.; Wang, D.H.; et al. Incorporation of gamma-aminobutyric acid and cesium cations to formamidinium lead halide perovskites for highly efficient solar cells. *J. Energy Chem.* **2022**, *64*, 561–567. [[CrossRef](#)]
5. Rasool, S.; Hoang, Q.V.; Van Vu, D.; Song, C.E.; Lee, H.K.; Lee, S.K.; Lee, J.C.; Moon, S.J.; Shin, W.S. High-efficiency single and tandem fullerene solar cells with asymmetric monofluorinated diketopyrrolopyrrole-based polymer. *J. Energy Chem.* **2022**, *64*, 236–245. [[CrossRef](#)]
6. Liu, W.S.; Huang, C.S.; Chen, S.Y.; Lee, M.Y.; Kuo, H.C. Investigation of $\text{Cu}_2\text{ZnSnS}_4$ thin film with preannealing process and ZnS buffer layer prepared by magnetron sputtering deposition. *J. Alloy. Compd.* **2021**, *884*, 161015. [[CrossRef](#)]
7. Zhang, H.Y.; Wei, Z.; Li, P.F.; Tang, Y.Y.; Xiong, R.G.J.A.C.I.E. The narrowest band gap ever observed in molecular ferroelectrics: Hexane-1,6-diammonium pentaiodobismuth(III). *Angew. Chem. Int. Ed.* **2018**, *57*, 526. [[CrossRef](#)] [[PubMed](#)]
8. Fabian, D.M.; Ardo, S. Hybrid organic–inorganic solar cells based on bismuth iodide and 1,6-hexanediammonium dication. *J. Mater. Chem. A* **2016**, *4*, 6837–6841. [[CrossRef](#)]
9. Liu, X.Y.; Zhang, G.H.; Zhu, M.J.; Chen, W.B.; Zou, Q.; Zeng, T. Polarization-enhanced photoelectric performance in a molecular ferroelectric hexane-1,6-diammonium pentaiodobismuth (HDA-BiI₅)-based solar device. *RSC Adv.* **2020**, *10*, 1198–1203. [[CrossRef](#)]
10. Jiang, Q.; Zhang, X.W.; You, J.B. SnO_2 : A wonderful electron transport layer for perovskite solar cells. *Small* **2018**, *14*, 1801154. [[CrossRef](#)]
11. Chen, Y.C.; Meng, Q.; Zhang, L.R.; Han, C.B.; Gao, H.L.; Zhang, Y.Z.; Yan, H. SnO_2 -based electron transporting layer materials for perovskite solar cells: A review of recent progress. *J. Energy Chem.* **2019**, *35*, 144–167. [[CrossRef](#)]
12. Nam, M.; Huh, J.Y.; Park, Y.; Hong, Y.C.; Ko, D.H. Interfacial modification using hydrogenated TiO_2 electron-selective layers for high-efficiency and light-soaking-free organic solar cells. *Adv. Energy Mater.* **2018**, *8*, 1703064. [[CrossRef](#)]
13. Nam, M.; Park, J.; Lee, K.; Kim, S.W.; Ko, H.; Han, I.K.; Ko, D.H. A multifunctional fullerene interlayer in colloidal quantum dot-based hybrid solar cells. *J. Mater. Chem. A* **2015**, *3*, 10585–10591. [[CrossRef](#)]
14. Ke, W.J.; Fang, G.J.; Liu, Q.; Xiong, L.B.; Qin, P.L.; Tao, H.; Wang, J.; Lei, H.W.; Li, B.R.; Wan, J.W.; et al. Low-temperature solution-processed tin oxide as an alternative electron transporting layer for efficient perovskite solar cells. *J. Am. Chem. Soc.* **2015**, *137*, 6730–6733. [[CrossRef](#)]
15. Yun, A.J.; Kim, J.; Hwang, T.; Park, B. Origins of efficient perovskite solar cells with low-temperature processed SnO_2 electron transport layer. *ACS Appl. Energy Mater.* **2019**, *2*, 3554–3560. [[CrossRef](#)]
16. Liu, X.; Tsai, K.W.; Zhu, Z.; Sun, Y.; Chueh, C.C.; Jen, A.K.Y. A Low-temperature, solution processable tin oxide electron-transporting layer prepared by the dual-fuel combustion method for efficient perovskite solar cells. *Adv. Mater. Interfaces* **2016**, *3*, 1600122. [[CrossRef](#)]
17. Jia, J.B.; Dong, J.; Wu, J.H.; Wei, H.M.; Cao, B.Q. Combustion procedure deposited SnO_2 electron transport layers for high efficient perovskite solar cells. *J. Alloy. Compd.* **2020**, *844*, 156032. [[CrossRef](#)]
18. Bai, G.F.; Wu, Z.L.; Li, J.; Bu, T.L.; Li, W.N.; Li, W.; Huang, F.Z.; Zhang, Q.; Cheng, Y.B.; Zhong, J. High performance perovskite sub-module with sputtered SnO_2 electron transport layer. *Sol. Energy* **2019**, *183*, 306–314. [[CrossRef](#)]

19. Xu, X.X.; Xu, Z.; Tang, J.; Zhang, X.Z.; Zhang, L.; Wu, J.H.; Lan, Z. High-performance planar perovskite solar cells based on low-temperature solution-processed well-crystalline SnO₂ nanorods electron-transporting layers. *Chem. Eng. J.* **2018**, *351*, 391–398. [[CrossRef](#)]
20. Saeed, M.A.; Kim, S.H.; Baek, K.; Hyun, J.K.; Lee, S.Y.; Shim, J.W. PEDOT:PSS: CuNW-based transparent composite electrodes for high-performance and flexible organic photovoltaics under indoor lighting. *Appl. Surf. Sci.* **2021**, *567*, 150852. [[CrossRef](#)]
21. Lee, J.H.; You, Y.J.; Saeed, M.A.; Kim, S.H.; Choi, S.H.; Kim, S.; Lee, S.Y.; Park, J.S.; Shim, J.W. Undoped tin dioxide transparent electrodes for efficient and cost-effective indoor organic photovoltaics (SnO₂ electrode for indoor organic photovoltaics). *NPG Asia Mater.* **2021**, *13*, 43. [[CrossRef](#)]
22. You, Y.J.; Saeed, M.A.; Shafian, S.; Kim, J.; Kim, S.H.; Kim, S.H.; Kim, K.; Shim, J.W. Energy recycling under ambient illumination for internet-of-things using metal/oxide/metal-based colorful organic photovoltaics. *Nanotechnology* **2021**, *32*, 465401. [[CrossRef](#)] [[PubMed](#)]